Spectroscopic Investigations of Poly(oxypropylene)glycol-Based Waterborne Polyurethane Doped with Lithium Perchlorate

Ten-Chin Wen* and Ming-Sieng Wu

Department of Chemical Engineering, National Cheng Kung University, Tainan, 701, Taiwan

Chien-Hsin Yang

Department of Environmental and Chemical Engineering, Kung Shan Institute of Technology, Tainan, Taiwan

Received March 23, 1998; Revised Manuscript Received January 25, 1999

ABSTRACT: Polyaddition of isophorone diisocyanate to poly(oxypropylene)glycol (PPG)-Based waterborne polyurethane (WPU) synthesized by a modified acetone process was performed. Fourier transform infrared spectroscopy (FTIR), X-ray photoelectron spectroscopy (XPS), differential scanning calorimetry (DSC), and impedance spectroscopy (IS) were utilized to monitor the phase change of this WPU with the doped lithium perchlorate ($LiClO_4$) concentration. Significant changes occur in the FTIR spectrum of the WPU with the added salt concentration above 1 mmol/g WPU, indicating that an interaction with the lithium cation within the hard segment and between the hard and soft phases occurs. The soft segment T_g increases with increasing $LiClO_4$ through the examination of DSC. XPS results reveal that the component of nitrogen polaron sites (N^+) increases with increasing $LiClO_4$ and that the saturation level of salt doping is evidenced by the mole ratio of component C−O to C═O; meanwhile, a rearrangement in the long chain of the soft domain has also been observed when this WPU is doped with $LiClO_4$. IS results indicate an increase in bulk conductivity as the salt concentration is increased.

Introduction

Since the discovery of poly(ethylene oxide) (PEO) electrolytes was first reported by Wright[1] and Armand et al.[2] in 1975, many researchers have studied the solid-state polymer electrolytes (SPE). Most of these researchers have concentrated on designing novel polymer materials which possess high ionic conductivity, mechanical strength, and thermal stability for technological applications.[3−6]

Among the various polymer electrolytes developed, polyether-based electrolytes showed desired features such as good adherence to the electrodes and the ability to dissolve many inorganic salts forming a homogeneous solution. The dissolution of alkali-metal salts in polyether polymers has been studied extensively.[7,8] The dissociation behavior of alkali−metal salts is characterized by the formation of transient cross-links between ether oxygens in the host polymer and alkali−metal cations; the anion is usually not solvated. Ionic transport is achieved through a coupling between the ions and polymer segmental motion; hence, to obtain high conductivity ($>10^{-5}$ S/cm), which is useful in ambient-temperature applications such as solid-state batteries[3] and fuel cells,[6] a polymer possessing high flexibility is required. On the other hand, solid polymer electrolytes are also necessary to exhibit excellent dimensional stability, having elastomeric properties in their service temperature range.[9] Ionic conductive polymers, such as complexes of PEI and lithium salt, have shown that ionic conduction occurs mainly in the amorphous domains of the polymer,[10] which possibly exhibits high ionic conductivity of 10^{-7}−10^{-8} S/cm at 60 °C. Unfortunately, PEI polymer readily crystallizes at ambient temperature. Therefore, many efforts have been made to increase the amorphous phase of the polymer by modifying its chemical structures.[11,12]

Thermoplastic polyurethanes (TPUs) are composed of a polyether or polyester soft segment and a diisocyanate-based hard segment, which can be characterized by a two-phase morphology.[13] The phase separation is due to the fact that the hard and soft phases are immiscible and leads to the formation of a hard-segment domain, a soft-segment matrix, and an ill-defined interphase. The hard-segment domains act as physical cross-links and filler particles to the soft-segment matrix. The domain formation is derived form the strong intermolecular hydrogen bonding between the hard−hard segments of urethane or urea linkages. Furthermore, several investigations have proved that there are some hard segments dissolved in the soft segment phase.[14−17] A number of parameters can influence the elastomeric properties of the TPU. The most significant ones are the kind of raw materials, the soft-segment molecular weight, and the hard-segment concentration.[18]

Infrared spectroscopy was employed extensively to study the hydrogen bonding and was a powerful tool in identifying the characteristics of hydrogen bonding.[15−17,19−34] The hydrogen bonding is characterized by a frequency shift to values lower than those corresponding to the free groups (i.e., no hydrogen bonding). Meanwhile, the extent of the frequency shift is usually used as an estimate of hydrogen-bonding strength. Particularly for polyether-based TPUs, the fraction of the hydrogen-bonded carbonyls is defined by a hard−hard segment hydrogen bond (NH···O═C bond), which was employed to evaluate the extent of phase separation. On the other hand, the fraction of the hydrogen-bonded ether oxygens (NH···O bond) represents the extent of phase mixing between hard and soft segments. Recently, several studies have attempted to elucidate the relationships between structure and properties

* Telephone: 886-6-2757575 ext. 62656. Fax: 886-6-2344496. E-mail: tcwen@mail.ncku.edu.tw .

10.1021/ma9804489 CCC: $18.00
Published on Web 03/25/1999

Scheme 1. Polymerization of PPG-Based WPU

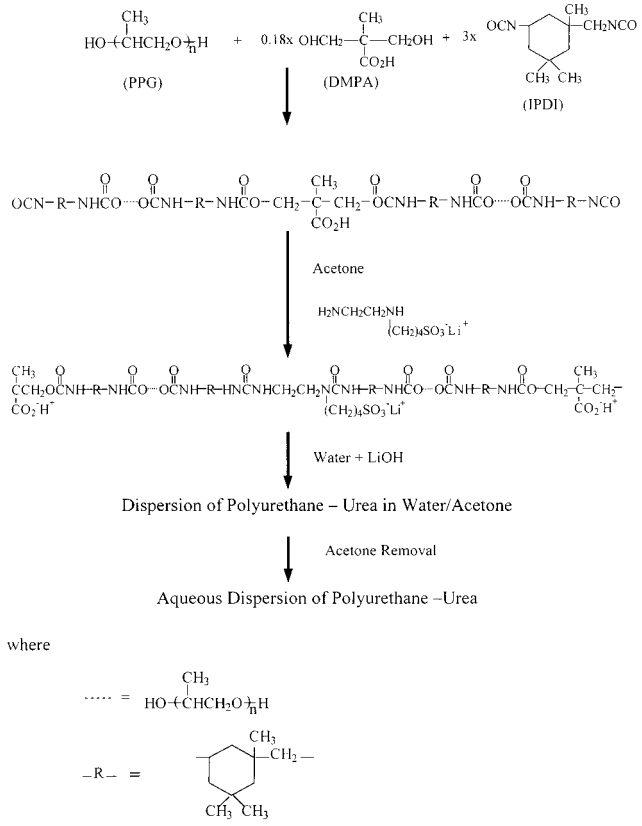

within TPUs using FTIR[19−34] and DSC.[35−38] Seki and Sato[39] and McLennaghan et al.[40,41] have proved that the doped lithium salt of TPUs results in an increase of the soft-segment T_g and a loss of the higher temperature endothermic transitions. More recently, Van Heumen and Stevens[33] have shown that the lithium salts of $LiCF_3SO_3$ and $Li(CF_3SO_2)_2N$ were observed to increase the overall bulk conductivity of a phase-segregated polyurethane comprising soft segments of poly(tetramethylene oxide) (PTMO) and hard segments of methylene-bis(phenyl isocyanate) (MDI) and 1,4-butanediol (BDO). Significant changes occur in the FTIR spectrum of the TPU when the critical salt concentration is above 0.5 mmol/g WPU, suggesting that an interaction with the lithium cation within the hard segment and between the hard and soft phase occurs. Thus, the characteristic phase-segregated morphology of the TPU has been altered as a result of the interaction of lithium cations within the polar hard domains and by the promotion of phase intermixing due to the coupling of the hard and soft phases.

Although many kinds of TPUs have been used as matrixes for ionic conduction, it is very laborious to make a film for practical applications. In this work, a poly(oxypropylene) glycol (PPG)-based waterborne polyurethane (WPU) was synthesized and used as a solid polymer electrolyte. By using FTIR, XPS, DSC and IS, we investigate the effect of the $LiClO_4$ concentration on the phase variation, surface characteristics, and bulk impedance of a WPU with a composition of IPDI/DMPA/PPG/ethylenediamine-derivative chain extender.

Experimental Section

Synthesis of WPU. WPU dispersions were prepared through our modified acetone process[49,50] as shown in Scheme 1 by polyaddition of isophorone diisocyanate (IPDI) to poly(oxypropylene)glycol and dimethylolpropionic acid (DMPA), followed by neutralization of pendant COOH with LiOH. The raw materials employed in this study are listed in Table 1. PPG was dried and degassed under vacuum at 70 °C for 2 days. DMPA was also dried under vacuum at 120 °C and then dissolved in DMF, which was distilled over anhydrous $MgSO_4$ at low pressure and stored over a 3 Å molecular sieve before use. The preparation of chain extender was similar to that in our previous paper[49] except for the use of LiOH instead of NaOH.

Table 1. Raw Materials

designation	chemical identification	suppliers
PPG	polypropylene glycol, $M_w = 1000$	Showa Chemicals, Inc.
IPDI	isophorone diisocyanate	Merck Co.
DMPA	dimethylol propionic acid	Aldrich Chemical, Inc.
DMF	dimethylformamide	Wako Chemical Co.
EDA	ethylenediamine	Merck
BS	butane sultone	Aldrich Chemical, Inc.
LiOH	lithium hydroxide	Merck Chemical, Inc.

Preparation of Polymer Film. WPU dispersion was poured on a Teflon disk at ambient conditions. After pouring, we allowed sufficient time to elapse for most of the water to evaporate, and the residual moisture was further removed by vacuum pumping at 60 °C for 3 days.

The desired lithium salt-doped polymer film was prepared by dissolving the cast film in acetone with proper $LiClO_4$/acetone solution. The solution was then cast under vacuum for 3 days at 60 °C to form 0, 1, and 2 mmol $LiClO_4$/g WPU polymer films doped as samples a, b, and c, respectively.

The films were then removed into a glovebox under vacuum for further drying. Before all tests of these films, the water content of these films was determined to be around 10 ppm with Karl Fisher moisture titrator (MKC-210, Kyoto Electronics, Japan).

Infrared Spectroscopy. Films for infrared analysis were prepared by casting 5% DMF solutions onto potassium bromide windows at room temperature. After the majority of the solvent evaporated, the films were placed in a vacuum oven at about 80 °C for over 24 h to remove residual solvent and moisture.

The films were then removed into a glovebox under vacuum for further drying. Before all tests of these films, the water content of these films was determined to be around 10 ppm Karl Fisher moisture titrator (MKC-210, Kyoto Electronics, Japan).

FTIR spectra were collected using a Nicolet 550 system at a resolution of 2 cm^{-1}, and a minimum of 64 scans were signal-averaged at room temperature. Band deconvolution of the resulting spectra was obtained by analysis with Grams 386 software (Galactic). The maximum error associated with the deconvolution of the IR spectra is expected to be ±5%. In most cases, the deconvolution was executed by fitting the spectra to different functions to ensure the accuracy of the deconvolution results.

DSC Thermograms. Thermal analysis of WPU was carried out using DSC (Du Pont 910, USA) over the range −100 to +150 °C at a heating rate of 20 °C/min. Sample was taken from WPU film and sealed in aluminum capsules for analysis.

X-ray Photoelectron Spectroscopy (XPS). The binding energy and atomic percentage were determined by XPS using an ESCA 210 spectrometer. The spectra employed Mg Kα ($h\nu$ = 1253.6 eV) irradiation as the photon source, with a primary tension of 12 kV and an emission current of 20 mA. Analysis chamber pressure during the scans was about 10^{-10} mbar.

Low-resolution survey scans were done at 50 eV pass energy, step 1 eV, to obtain the atomic percentage data. After the survey spectra were obtained, higher resolution survey scans were performed at a pass energy of 20 eV, step 200 meV, with at least 10 scans. Subpeaks were deconvoluted using a curve-fitting method.

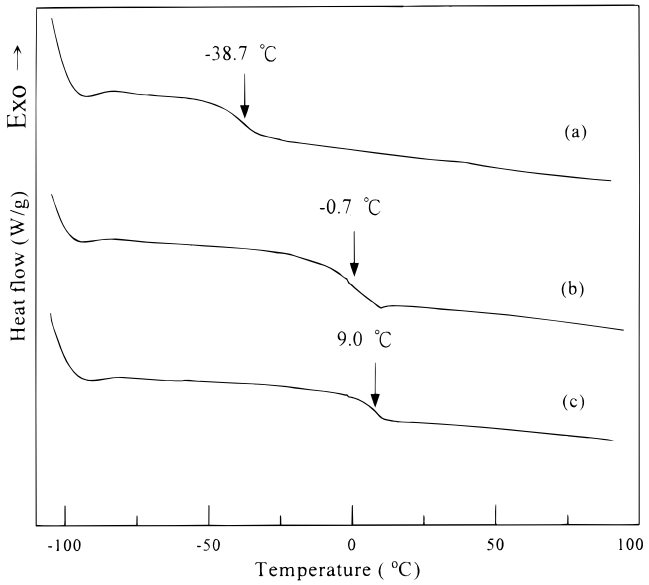

Figure 1. DSC thermograms for WPU doped with various $LiClO_4$ concentrations: (a) 0, (b) 1, and (c) 2 mmol/gWPU.

Impedance Spectroscopy. Impedance measurements were performed using thin films prepared previously of about 200 μm in thickness and 0.785 cm^2 in area. The ionic conductivity of the WPU films sandwiched between two stainless steel electrodes was obtained by using CMS300 EIS (Gamry Instruments, Inc., USA) together with an SR810 DSP lock-in amplifier (Stanford Research Systems, Inc., USA) under an oscillation potential of 10 mV from 100 kHz to 0.1 Hz.

Results and Discussion

DSC. DSC was utilized to examine the effect of $LiClO_4$ on the polyether soft-segment T_g of the WPU. Figure 1 shows that the T_g of the PPG soft-segment is increased by increasing the salt concentration. This is consistent with previous investigations of $LiClO_4$-doped TPUs containing either PEO[40,41] or PPO[42,43] as the soft-segment. It is also corroborated by the report that T_g increases with increasing salt concentration for polyether complexes with $LiCF_3SO_3$.[44] This indicates that the solvation of the lithium cation by the PPO soft segment partially arrests the local motion of the polymer segment through the formation of transient cross-links, leading to an increase in the soft-segment T_g. By normalizing T_g data against salt concentration, $\Delta T_g/\Delta C$ was calculated at each measurement, and it is obvious that a nonlinear increase in T_g is observed with increasing salt concentration. Actually, the value of $\Delta T_g/\Delta C$ decreases at high salt concentrations (Figure 1). This situation is attributable to the plasticizing effect generated by the formation of charge-neutral contact ion pairs with increasing salt concentration.[45] The neutral contact ion pairs lose the ability to provide ionic cross-links; hence, the further increase in T_g is insignificant.

Infrared Analysis. FTIR was utilized at ambient temperature (25 °C) to study the effect of salt concentration on the phase morphology of the WPU. Two major spectrum regions in this work are of the main interest: the NH stretching vibration at 3000−3650 cm^{-1} and the carbonyl stretching vibration at 1600−1800 cm^{-1}. To directly study the extent and strength of hydrogen bonding in both hard−hard and hard−soft segments, experiments were performed to analyze the infrared absorption of the two spectral regions by varying the salt concentration.

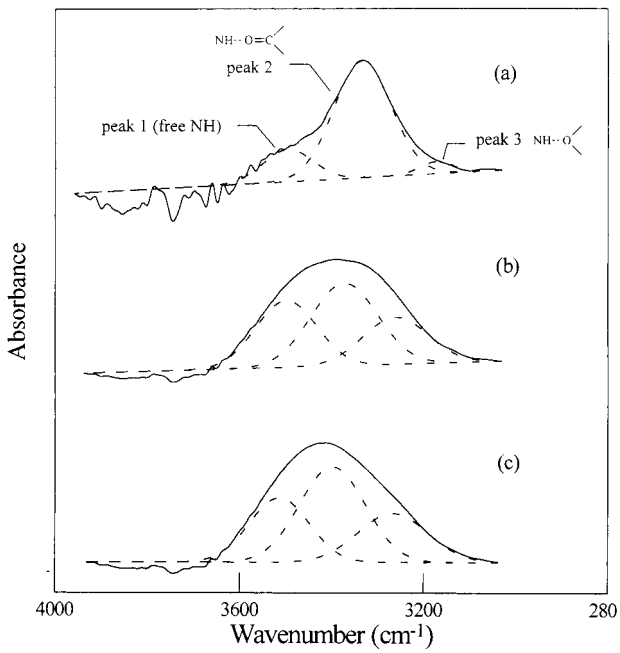

Figure 2. Decomposition of N−H stretching for WPU doped with various $LiClO_4$ concentrations: (a) 0, (b) 1, and (c) 2 mmol/g WPU.

Table 2. Decomposition Results of the N−H Stretching

	peak position			peak area (%)[a]		
film	1	2	3	1	2	3
a	3493	3334	3170	18.3	77.1	4.6
b	3498	3375	3263	32.3	43.8	23.9
c	3518	3396	3273	28.5	46.7	24.8

[a] The peak areas are based on total N−H stretching band area.

NH Stretching Region. Figure 2 shows the IR spectra of the NH stretching region with external doping salt concentration ranging from 0 to 2 mmol $LiClO_4$/g WPU. In each spectrum, the NH stretching vibration exhibits a strong absorption peak centered at around 3330−3400 cm^{-1} arising from the hydrogen bonding between NH and carbonyl groups, whereas the free NH stretching vibration appears at ca. 3493−3520 cm^{-1}. Note that there appears another obvious shoulder or peak at ca. 3170−3275 cm^{-1}. This peak corresponds to the NH···O hydrogen bonding which is established on the basis of the previously evidenced existence of the NH stretching vibration at ca. 3258−3295 cm^{-1}.[26] This result is attributable to the phase-mixed state between hard and soft segment via hydrogen bonding in the polymers.

Deconvolution of the NH stretching region was found to the best fits by using a Gaussian−Lorentzian sum. The maximum frequency (ν) and area of each band were determined by using the Nelder−Mead optimization method. As shown previously by many researchers,[25,26] the typical free NH band at ca. 3440 cm^{-1} appears as a low-intensity shoulder on the measured TPUs. The position of the free NH band was higher than 3490 cm^{-1} with a high salt concentration. This indicates that the free NH stretching vibration peak 1 is enhanced due to the increase in salt concentration. All NH band areas were normalized on the basis of total N−H stretching band area and are listed in Table 2. Both band shift and band area of free NH stretching are approximately proportional to salt concentration. The band shift in this

Scheme 2. Schematics for the Suggested Coordination of Lithium Salt with PPG-Based WPU

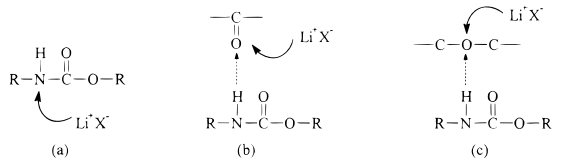

work is presumably due to the interaction between the Li^+ cation and the lone pair of electrons on the nitrogen atom,[46] leading to N−H bond length be reduced as seen in Scheme 2a.

The band of hydrogen bonding between NH and carbonyls (peak 2) was shifted from 3334 cm^{-1} for the WPU with the lowest salt content to 3396 cm^{-1} for that with the highest salt content. Because band position is related to the strength of the H-bonded NH band, then the shift to higher frequency with increasing salt concentration indicated an increase in the bond strength of the N−H bond. This is likely due to the localization of the electron-rich oxygens through coordination of the Li^+ cation with the hydrogen-bonded species (see Scheme 2b). Thus the strength of the hydrogen bonding between NH and carbonyls is weakened, resulting in the shift to higher frequency for the NH band affected by carbonyls. In addition, the band area (peak 2) decreased with increasing salt concentration in Table 2. This result provides the evidence that the possibility of the hydrogen bonding between NH and carbonyls is decreased.

Notice that Table 2 reveals the band position of hydrogen bonding of NH to ether oxygens (peak 3) of PPG soft segment was shifted from 3170 cm^{-1} in the lowest doped WPU, to 3273 cm^{-1} at the highest salt concentration. This shift of frequency to higher values increases with increasing salt concentration, implying that increased amounts of lithium salt in WPU give a stronger band strength of the N−H bond. This is likely due to the coordination of nonbonded electrons on the ether oxygens with the Li^+ cation, leading a weakening of the hydrogen-bonded strength between NH and ether oxygens (see Scheme 2c). An examination of Table 2 reveals that the band area of NH−ether (peak 3) increases with increasing salt concentration. This is attributed to the fact that the coordination of nonbonded electrons on ether oxygens with Li^+ cation is increased, inducing an increase hydrogen bonding between NH and ether groups.

An ether oxygen atom−Li^+ cation coordinate bond is formed with the addition of salt, and this formation of coordination bond will induce the hydrogen bonding of NH to ether oxygens. The inductive effect of hard−soft segments occurs more significantly than that of hard−hard segment, which is increased with increasing salt concentration.

C═O Stretching Region. Figure 3 shows the IR spectra of the carbonyl stretching region for the three WPU samples. The band centered at around 1725 cm^{-1} is attributed to the stretching of free urethane carbonyl groups, whereas the band at 1713 cm^{-1} is assigned to hydrogen-bonded urethane carbonyl groups. Previous studies[20,28] concluded that the urethane carbonyl stretch at around 1710 cm^{-1} is due to hydrogen bonding in disordered regions, corresponding to carbonyl participating in urethane linkage of interfacial regions or being "dissolved" in the soft phase. For the stronger hydrogen bonds in ordered or crystalline regions, the stretching absorbance occurs at a lower frequency at ca. 1695 cm^{-1}.

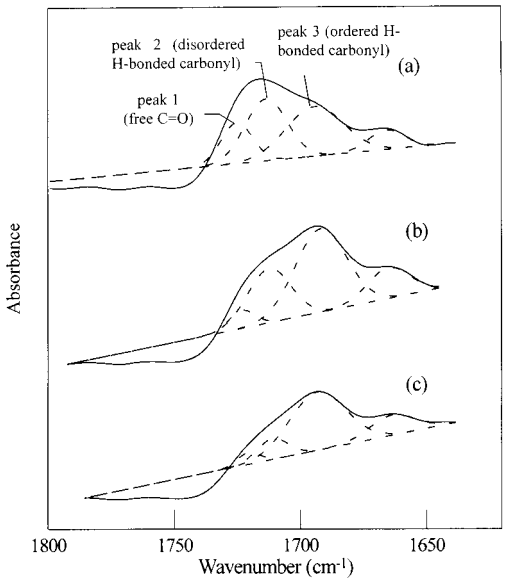

Figure 3. Decomposition of C═O stretching for WPU doped with various $LiClO_4$ concentrations: (a) 0, (b) 1, and (c) 2 mmol/g WPU.

Table 3. Decomposition Results of the C═O Stretching

	peak position			peak area (%)[a]		
film	1	2	3	1	2	3
a	1725	1713	1694	19.1	38.6	42.3
b	1723	1712	1692	6.6	33.2	60.2
c	1721	1711	1693	6.2	15.6	78.2

[a] The peak areas are based on total C═O stretching band area.

The band centered at ca. 1665 cm^{-1} is assigned to the stretching of hydrogen-bonded carboxylic carbonyl group, which comes from DMPA unit.

The deconvolution of the carbonyl region by a Gaussian function was also performed and listed in Table 3. The stretching of free urethane carbonyl shifts from 1725 to 1721 cm^{-1} when salt concentration is increased from 0 to 2 mmol/g WPU. This shift to a lower frequency suggests that the ionic coordination between the free urethane carbonyl and Li^+ cation increases with increasing salt concentration. The areas of the free urethane carbonyl groups decrease with increasing salt concentration. This is attributable to the fact that the ionic coordination between free urethane carbonyl and Li^+ increases with increasing salt concentration, leading to a decrease in the amount of free urethane carbonyl.

The stretching vibration band of disordered hydrogen-bonded urethane carbonyl occurs at 1713 ± 2 cm^{-1}, nearly independent of salt concentration. The area of the disordered H-bonded urethane carbonyl decreases with increasing salt concentration. From DSC results, an increase in soft-segment T_g with increasing salt concentration indicates that the solvation of the lithium cation by PPG soft segment partially arrests the local motion of the polymer segments through transient cross-links. Thereby, the amount of disordered hydrogen-bonded urethane carbonyl which participates in urethane linkage of interfacial regions or is dissolved in the soft phase will be reduced. The band position of ordered hydrogen-bonded urethane carbonyl is nearly constant (1695 ± 2 cm^{-1}).

The area of the ordered H-bonded urethane carbonyl increases with increasing salt concentration. The decrease in the amount of disordered hydrogen-bonded

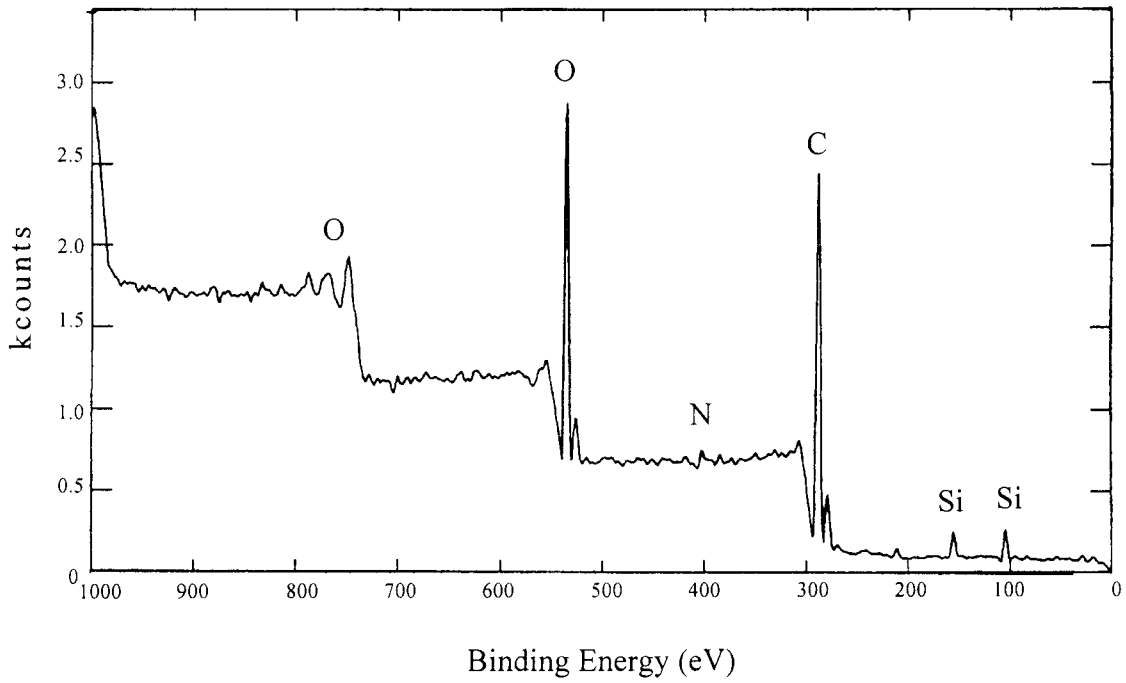

Figure 4. Wide scan XPS of 0 mmol $LiClO_4$/g WPU (sample a).

Table 4. Surface Elemental Makeup of PPG-Based WPU

					C_{1s}			O_{1s}				N_{1s}						
sample	atom percent (%)				C=O	C−O	C−C	C=O	C−O	Si−O	D[a]−O	N^+	−NH−	−N=			C−C/C−O (carbon ratio)	C−O/C=O (oxygen ratio)
B.E.[b]	C_{1s}	N_{1s}	O_{1s}	Si_{2p}	288.8	286.1	284.6	534.0	531.5	532.5	529.3	401.2	399.9	398.9	O/C	N/C		
a	71.1	1.9	21.1	5.9	2.8	35.2	62.0	2.1	6.2	88.6	3.1	2.3	87.9	9.8	0.30	0.026	1.76	2.95
b	57.2	1.0	18.9	22.9	2.4	42.9	54.7	1.7	4.6	92.5	1.2	3.3	85.4	11.3	0.33	0.017	1.28	2.71
c	61.4	1.6	19.7	17.3	3.2	32.7	64.1	4.2	38.8	56.0	1.0	4.4	93.7	1.9	0.32	0.026	1.96	9.24

[a] Salt anions containing both ClO_4^- and SO_3^-. [b] Binding energy (eV).

urethane carbonyl will partially be transformed into ordered hydrogen-bonded urethane carbonyl through the rearrangement of urethane linkage (orientation). It results in an increase of ordered hydrogen-bonded urethane carbonyl with increasing salt concentration.

As compared with the NH stretching region, the frequencies of the vibrations in the carbonyl stretching region do not shift as much because of the vibration of the salt concentration, and the absorption coefficient (e) is not related to frequency. The band area changes of the urethane carbonyl region are therefore directly related to a decrease in the fraction of free urethane carbonyls (X_F) with increasing salt concentration. The fraction of free and hydrogen-bonded urethane carbonyl groups can be approximately approached by the following relationship. The total concentration of carbonyl groups is given by[34]

$$C_T = C_F + C_B \quad (1)$$

where C_F and C_B are the concentration of free and hydrogen-bonded urethane carbonyl groups, respectively. The fraction of hydrogen-bonded urethane carbonyl is given by

$$X_B = C_B/C_T \quad (2)$$

The results of X_B are 0.81, 0.93, and 0.94 for samples a, b, and c, respectively. It is obvious that X_B gradually increases with increasing the salt concentration. It suggests that the concentration of hydrogen-bonded urethane carbonyls is increased with increasing $LiClO_4$. To identify the resultant state of the polymer surface, XPS is used for chemical analysis in the next section.

Chemical Analysis. Low-resolution wide scanning provides a determination of which elements were present in a WPU. A typical XPS survey scan of the polymer with 1 mmol $LiClO_4$/g WPU external doping salt concentration is shown in Figure 4, revealing that C, N, O, and Si signals are detected in this polymer sample. All samples analyzed contained some amount of silicon contaminant. The amounts of Cl, S, and Li are too small to be detected. The relative concentrations of C, N, O, and Si in the polymer film, calculated from the corresponding photoelectron peak area after sensitivity factor corrections (SF = 1.00, 1.77, 2.85, and 0.87 for C_{1s}, N_{1s}, O_{1s} and Si_{2p}, respectively), are listed in Table 4. It should be noted that carbon and oxygen were the dominant elements detected on the surfaces of all samples; a small amount of nitrogen in the hard segment phase was also detected. An examination of Table 4 reveals that there exist different values of O/C, N/C, and C−C/C−O carbon ratios in the three samples. This suggests that the lithium salt doped into WPU films may have altered the chemical structure of the material surface. The values of O/C ratios are higher than those of N/C, indicating that the soft segment phase is more preferentially presented on the surface of these samples than the hard segment phase. The values of O/C ratios essentially increase with increasing $LiClO_4$, implying that the samples doped with external salt generate greater proportions of soft segments on the surface than the sample not doped with external

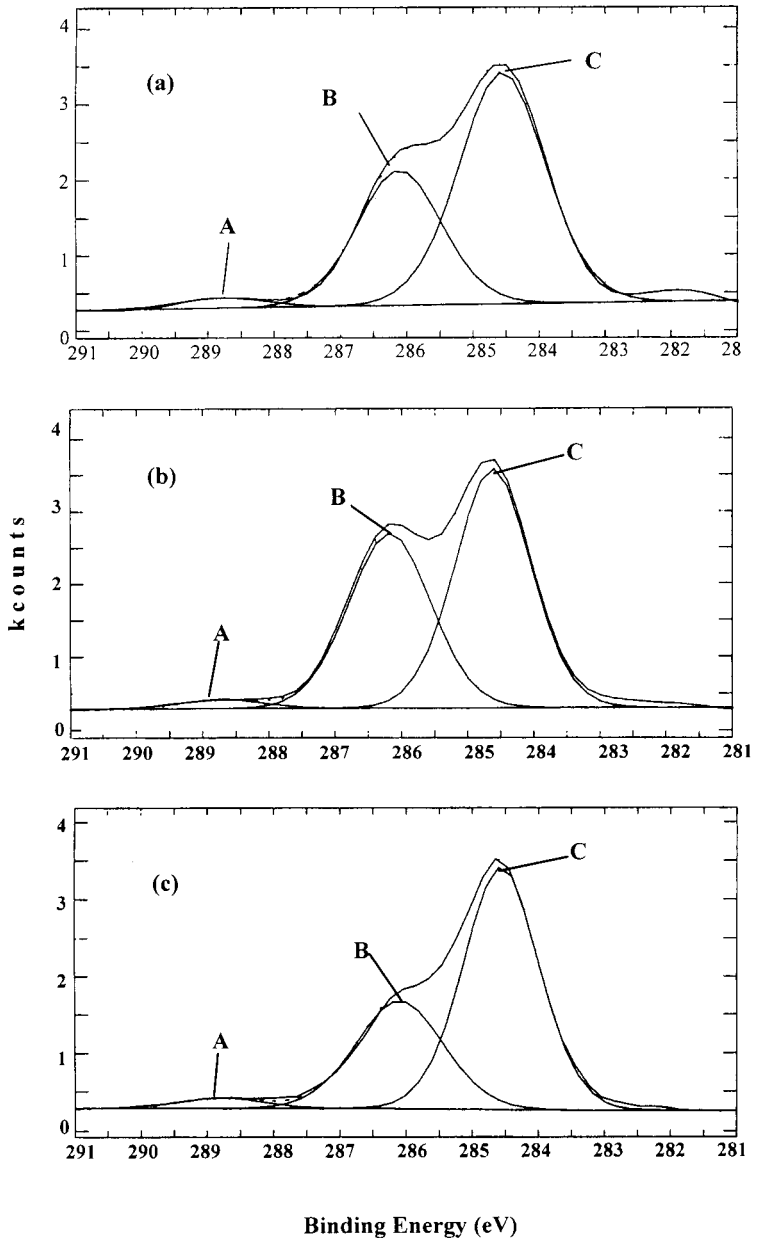

Figure 5. C_{1s} XPS core-level spectra of WPU doped with various $LiClO_4$ concentrations: (a) 0, (b) 1, and (c) 2 mmol/g WPU.

salt. Because nitrogen only exists in the hard segment, the ratio of N_{1s} to C_{1s} corresponds to the relative surface concentration of hard segments. Only one of the samples, b (1 mmol $LiClO_4$/g WPU), did have the decreased N/C ratio. This result implies that the sample doped with external salt from 0 to 1 mmol/g WPU possesses significantly decreased proportions of hard segments on the surface in comparison to the undoped sample, a. Rearrangement of the hard segments to the WPU surface is facilitated by a small doping amount of external salt. In this case, the rearrangement of the hard segments due to external doping would be correlated by the increase in soft-segment T_g of WPU. As the external salt concentration is increased to 2 mmol/g WPU (sample c), the surface of WPU sample has a N/C ratio of 0.026 which is the same as the undoped WPU (sample a), indicating that this sample had an increased proportion of hard segments on the surface in comparison to sample b. This result suggests that a N/C ratio of 0.026 exists as a saturated and stable orientation (architecture) of polymer linkages.

From C_{1s} core-level spectra of the three polymer films in Figure 5, three C_{1s} component peaks were identified at 285.0, 286.5, and 289.0 eV as small shoulders. The major C_{1s} peak at 285.0 eV corresponds to the aliphatic carbon, whereas the peak at 286.5 eV corresponds to the ether carbon of the polyether soft segment. The small peak at 289.0 eV corresponds to the carbonyl carbon derived from the urea and urethane linkages.[47] It was particularly evident for sample b which demonstrated a significant reduction in the relative amount of C−C content and the increase in the amount of C−O content, whereas sample a showed a significant reduction in the amount of C−O content and an increase in the amount of C−C content. This relative change is illustrated in Figure 5, which is used to compare the undoped and doped WPU samples. The sensitive C_{1s} core-level can be accurately resolved into contributions from C−C (hydrocarbon), C−O (ether), and C═O (urea and urethane). This analysis, also shown in Table 4, gave a relative decrease in C−C and an increase in C−O for sample b in comparison to sample a. Note that there

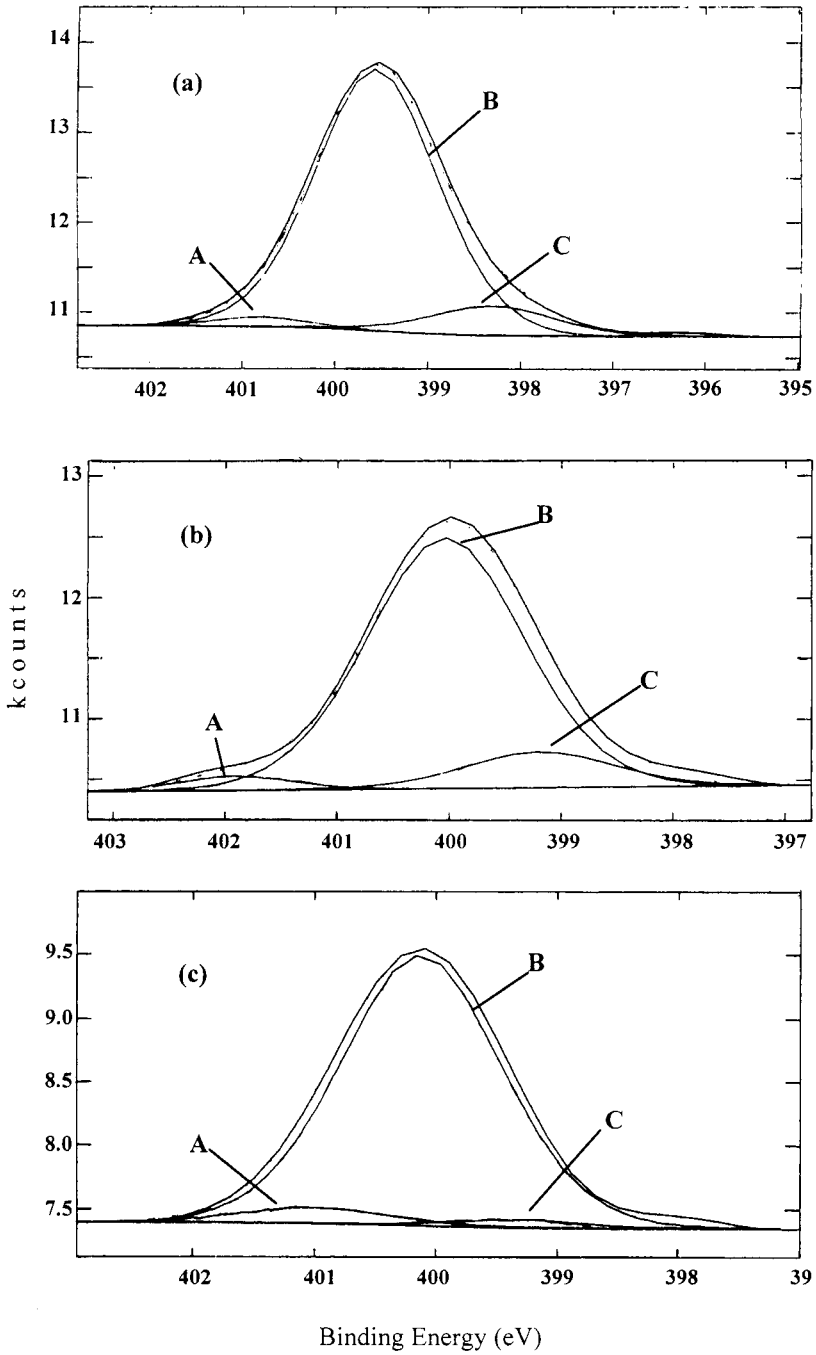

Figure 6. N_{1s} XPS core-level spectra of WPU doped with various $LiClO_4$ concentrations: (a) 0, (b) 1, and (c) 2 mmol/g WPU.

is no significant increase in C−O for sample c which has a high C−C/C−O carbon ratio. This implies that a high O/C ratio should come from the doped ClO_4^- anions in the sample c.

The N_{1s} core-level spectra of the three WPU samples have also been deconvoluted by assigning binding energies of 399.1, 400.1, and 402.0 eV for the −N═ (imine site), −NH− (amine site), and N^+ (polaron site) species, respectively,[48] as illustrated by the spectra in Figure 6. Note that the second component peak (amine site) is dominant in the N_{1s} core-level spectrum of these films. This is derived from the urea and urethane linkages. The formation of N^+ polaron is due to the nitrogen in the vicinity of Li^+ cations when the WPU samples were doped with $LiClO_4$. On the other hand, the imine site arises from the strong hydrogen bonding of −NH to O═C or −O− groups. The decomposition of the N_{1s} core level for the three WPU samples is also listed in Table 4. From Table 4, the concentration of N^+ component increases with increasing salt concentration. It is reasonable that the concentration of Li^+ cations increases with increasing salt concentration, and the increase results in a higher probability of nitrogen attaching to the Li^+ cation. As the external salt increased from 0 to 1 mmol/g WPU, the imine site increases with increasing salt concentration. This suggests that the strong hydrogen bonding is enhanced by the addition of salt, whereas the component of the amine site is relatively reduced. In contrast, for the highest salt-doped sample c, the component of the imine site is less than that of other two samples (samples a and b) and is shifted to the amine component. This result reflects that the strong hydrogen bonding is weakened

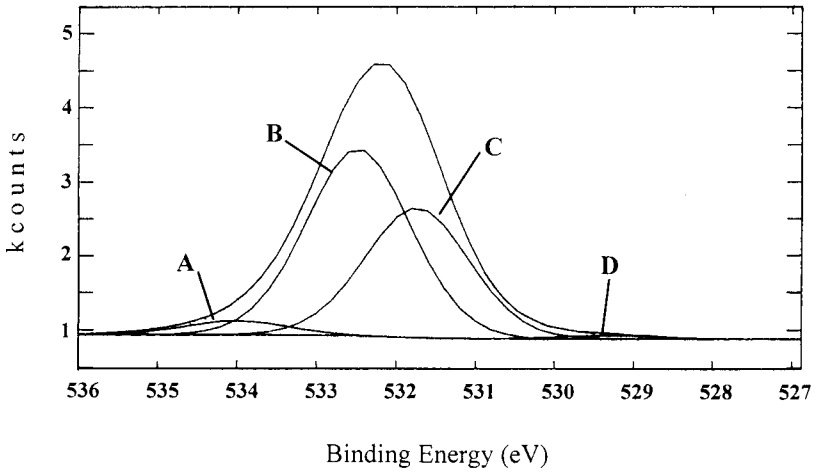

Figure 7. Typical O_{1s} XPS core-level spectra of WPU doped with various $LiClO_4$ concentrations: (a) 0, (b) 1, and (c) 2 mmol/g WPU.

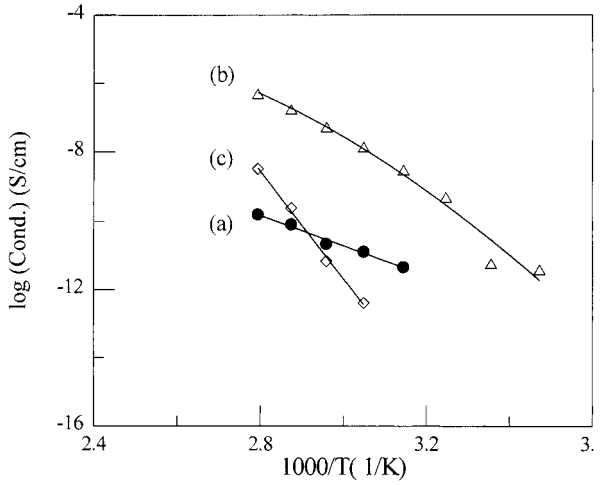

Figure 8. Dependence of conductivity on the reciprocal of temperature for WPU doped with various $LiClO_4$ concentrations: (a) 0, (b) 1, and (c) 2 mmol/g WPU.

by reaching the saturation level for the external doped salt.

The O_{1s} core-level spectra of the three WPU samples have been deconvoluted by assigning binding energies of 534.0, 532.5, 531.7, and 529.3 eV for the C═O, Si−O, C−O, and ClO_4^- (coupled with SO_3^-) species, respectively,[47] as illustrated by the spectra in Figure 7. The decomposition of the O_{1s} core level for the three WPU samples is also listed in Table 4. An examination of Table 4 reveals that the ratio of component of C−O to C═O for oxygen is smaller for sample b (1 mmol $LiClO_4$/g WPU) than that for sample a (undoped $LiClO_4$) and is much higher for sample c (doped with 2 mmol $LiClO_4$/g WPU) than those of samples a and b. The former result can be ascribed to the unsaturated doping level of the lithium salt, resulting in C═O site being preferentially attached to lithium cations. This mainly follows the mode b in Scheme 2. The latter result can be attributable to the saturated doping level of the lithium salt being reached, leading to C−O sites being doped afterward by lithium cations. This can be explained as mode c in Scheme 2.

Conductivity Analysis. It is interesting to investigate the conductivity of WPU-based electrolytes because of our previous work.[51] Figure 8 illustrates the temperature dependence of ionic conductivity for the $LiClO_4$/WPU complex. From an examination of this figure, it is evident that the bulk conductivity does not significantly increase with increasing doped salt concentration. Similar to that observed by McLennaghan et al.,[41] a maximum conductivity is observed as a function of concentration over the entire temperature; there exists a maximum conductivity for sample b in our case. It should be noted that the conductivity of sample c is lower than that of sample b over the entire temperature range. This result indicates that the bulk conductivity significantly rises with increasing external salt concentration from 0 to 1 mmol $LiClO_4$/g WPU. This reflects that the lithium salt-doped level of sample b is not yet saturated. Thus, the ionic conductivity data for sample b in Figure 8 was analyzed by using the Vogel−Tamman−Fulcher (VTF) relationship as follows:

$$\sigma(T) = AT^{-1/2} \exp[-B/k_B(T - T_0)] \qquad (3)$$

The application of the VTF form to ion transport in polymer electrolytes requires a coupling of mobile charge carriers to the segmental motion of the polymer host.[33] It can be evidenced that for sample b (unsaturated salt level), the ions are predominantly coupled to the segmental motions of the host polymer because the VTF form provides the best fit.

Also note that the conductivity of sample c is still higher than that of sample a at temperatures above 70 °C but lower below 70 °C. These results can be explained as follows: (i) the formation of ion pair increases with the alkali−metal salt concentration,[45] which limits the mobility of the charge carriers in the polymer matrix, resulting in lower bulk conductivity; (ii) a considerable amount of salt is interacting or coordinating with the hard domain as reflected by the FTIR results. These phenomena mainly exist in sample c at temperatures below 70 °C. In this situation, the salt is unable to participate in the conductive process until the temperature region of the hard segment T_g (≈80 °C) is reached.

The conductivity data for sample c as shown in Figure 8 was analyzed using the Arrhenius phenomenological relationship as follows:

$$\sigma(T) = A \exp[-E/k_B T] \qquad (4)$$

The Arrhenius form is used when the ions are decoupled from the polymer host and activated hopping is required for ionic transport. For sample c, it can be seen that

the Arrhenius form gives the best fit, and therefore, activated hopping predominates in the process.

Conclusions

A PPG-based waterborne polyurethane was successfully synthesized by the modified acetone process. This polymer exhibits partial phase mixing which is evidenced by the solution of soft segments in the hard-segment domains and hard segments in the soft-segment domains. Specific interactions between the lithium cation and the electron-rich components (e.g., nitrogen and oxygen) of the urethane moiety have been examined via the application of FTIR and XPS. In addition, it can also conclude that this PPG-based WPU is a suitable polymer host for preparing a solid polymer electrolyte having a moderately high conductivity and dimensional stability.

Acknowledgment. The authors are grateful to the National Science Council in Taiwan for its financial support through NSC 87-2214-E-006-026.

References and Notes

(1) Wright, P. V. *Brit. Polym. J.* **1975**, *7*, 319.
(2) Armand, B. M. In *Fast Ion Transport in Solids*; van Gool, W., Ed.; North-Holland: Amsterdam, 1973; p 665.
(3) Gauthier, M.; Belanger, A.; Kapper, B.; Vassort, G.; Armand, M. *Polymer Electrolytes Review 2*; MacCallum, J. R., Vincent, C. A., Eds.; Elsevier: London, 1989; p 285.
(4) Anderson, A. M.; Stevens, J. R.; Granqvist, C. G. *Large Area Chromogenics-Materials and Devices for Transmittance Control*, Vol. IS4; Lambert, C. M., Granqvist, C. G., Eds.; Institute Series; Opt. Eng. Press: Bellingham, WA, 1990; p 471.
(5) Hrai, Y.; Tapi, C. *Appl. Phys. Lett.* **1983**, *43*, 704.
(6) Przyluski, J.; Wieczorek, W. *Synth. Met.* **1991**, *45*, 323.
(7) Armand, M. B.; Chabagno, J. M.; Dudot, M. J. *Fast Ion Transport in Solids*; Vashista, P.; Mundy, J. N., Shenoy, G. K., Eds.; Elsevier-North-Holland: New York, 1979; p 131.
(8) Fenton, D. E.; Parker, D. E.; Wright, P. V. *Polymer* **1973**, *14*, 589.
(9) Ratner, M. A.; Shriver, D. F. *Chem. Rev.* **1988**, *88*, 109.
(10) Harris, C. S.; Shriver, D. S.; Ratner, M. A. *Macromolecules* **1986**, *19*, 987.
(11) Gray, F. M. *Solid Polymer Electrolytes-Fundamentals and Technological Applications*; VCH: Weinheim, Germany, 1991; Chapter 6.
(12) Cheradame, H.; LeNest, J. F. *Polymer Electrolyte Reviews 1*; MacCallum, J. R., Vincent, C. A., Eds.; Elsevier: London, 1987; p 103.
(13) Van Bogart, J. V.; Gibson, P. E.; Cooper, S. L. *J. Polym. Sci., Polym. Phys. Ed.* **1983**, *21*, 65.
(14) Koberstein, J. T.; Russell, T. P. *Macromolecules* **1986**, *19*, 714.
(15) Wang, C. B.; Cooper, S. L. *Macromolecules* **1983**, *16*, 775.
(16) Coleman, M. M.; Skrovanek, D. J.; Hu, J.; Painter, P. C. *Macromolecules* **1988**, *21*, 59.
(17) Seymour, R. W.; Estes, G. M.; Cooper, S. L. *Macromolecules* **1970**, *3*, 579.
(18) Seefried, C. G., Jr.; Koleske, J. V.; Critchfield, F. E. *J. Appl. Polym. Sci.* **1975**, *19*, 2493.
(19) Sung, C. S. P.; Schneider, N. S. *Macromolecules* **1975**, *8*, 68.
(20) Sung, C. S. P.; Schneider, N. S. *Macromolecules* **1977**, *10*, 452.
(21) Senich, G. A.; MacKnight, W. J. *Macromolecules* **1980**, *13*, 106.
(22) Sung, C. S. P.; Smith, T. W.; Sung, N. H. *Macromolecules* **1980**, *13*, 117.
(23) Sung, C. S. P.; Hu, C. B. *Macromolecules* **1981**, *14*, 212.
(24) Brunette, C. M.; Hsu, S. L.; MacKnight, W. J. *Macromolecules* **1982**, *15*, 71.
(25) Coleman, M. M.; Lee, K. H.; Skrovanek, D. J.; Painter, P. C. *Macromolecules* **1986**, *19*, 2149.
(26) Lee, H. S.; Wang, Y. K.; Hsu, S. L. *Macromolecules* **1987**, *20*, 2089.
(27) Lee, S. S.; Wang, Y. K.; MacKnight, W. I.; Hsu, S. L. *Macromolecules* **1988**, *21*, 270.
(28) Pollack, S. K.; Shen, D. Y.; Hsu, S. L.; Wang, Q.; Stidham, H. D. *Macromolecules* **1989**, *22*, 551.
(29) Lee, H. S.; Hsu, S. L. *Macromolecules* **1989**, *22*, 1100.
(30) Yoon, S. C.; Sung, Y. K.; Ratner, B. D. *Macromolecules* **1988**, *21*, 59.
(31) Zharkov, V. V.; Strikovsky, A. G.; Verteletskaya, T. E. *Polymer* **1993**, *34*, 938.
(32) Wang, F. C.; Feve, M.; Lam, T. M.; Pascault, J. P. *J. Polym. Sci., Part B: Polym. Phys.* **1994**, *32*, 1305.
(33) Van Heumen, J. D.; Stevens, J. R. *Macromolecules* **1995**, *28*, 4268.
(34) Teo, L. S.; Chen, C. Y.; Kuo, J. F. *Macromolecules* **1997**, *30*, 1793.
(35) Seymour, R. W.; Cooper, S. L. *Macromolecules* **1973**, *6*, 48.
(36) Hesketh, T. R.; Van Bogant, J. W. C.; Cooper, S. L. *Polym. Eng. Sci.* **1980**, *20*, 190.
(37) Koberstein, J. T.; Galambos, A. F. *Macromolecules* **1992**, *25*, 5618.
(38) Leung, L. M.; Koberstein, J. T. *Macromolecules* **1986**, *19*, 706.
(39) Seki, M.; Sato, K. *Macromol. Chem.* **1992**, *193*, 2971.
(40) McLennaghan, A. W.; Pethrick, R. A. *Eur. Polym. J.* **1988**, *24*, 1063.
(41) McLennaghan, A. W.; Hooper, A.; Pethrick, R. A. *Eur. Polym. J.* **1989**, *25*, 1297.
(42) Watanabe, M.; Dohashi, S.; Sanui, K.; Ogata, N.; Kobayashi, T.; Ohtaki, E. *Macromolecules* **1985**, *18*, 1945.
(43) Watanabe, M.; Sanui, K.; Ogata, N. *Macromolecules* **1986**, *19*, 815.
(44) Albinsson, I.; Mellander, B. E.; Stevens, J. R. *J. Chem. Phys.* **1992**, *96*, 681.
(45) Schantz, S.; Torell, L. M.; Stevens, J. R. *J. Chem. Phys.* **1991**, *94*, 6862.
(46) Lu, X.; Weiss, R. A. *Macromolecules* **1991**, *24*, 4381.
(47) Stevenson, J. S.; Kusy, R. P. *J. Mater. Sci.: Mater. Med.* **1995**, *6*, 377.
(48) Yue, J.; Epstein, A. *J. Macromolecules* **1991**, *24*, 4441.
(49) Yang, C. H.; Lin, S. M.; Wen, T. C. *Polym. Eng. Sci.* **1995**, *35*, 722.
(50) Yang, C. H.; Li, Y. J.; Wen, T. C. *Ind. Eng. Chem.* **1997**, *36*, 1614.
(51) Cheng, T. T.; Wen, T. C. *Solid State Ionics* **1998**, *107*, 161.

MA9804489